

## Optimization of Adsorption Parameters for Reactive Red 4 (RR4) Removal by Cross-linked Chitosan-Epichlorohydrin using Box-Behnken Design

Nurul Najwa Abd Malek<sup>1</sup>, Emad Yousif<sup>2</sup>, Ali H. Jawad<sup>1\*</sup>

<sup>1</sup>Faculty of Applied Sciences, Universiti Teknologi MARA, 40450 Shah Alam, Selangor, Malaysia

<sup>2</sup>Department of Chemistry, College of Science, Al-Nahrain University, Baghdad, Iraq

Corresponding author: [ali288@uitm.edu.my](mailto:ali288@uitm.edu.my)

Received: 1 July 2019; Accepted: 25 August 2019; Published: 31 January 2020

### ABSTRACT

Cross-linked chitosan-epichlorohydrin was prepared for the adsorption of Reactive Red 4 (RR4). Response surface methodology (RSM) with 3-level Box-Behnken design (BBD) was employed to optimize the RR4 dye removal efficiency from aqueous solution. The adsorption key parameters that were selected such as adsorbent dose (A: 0.5 – 1.5 g), pH (B: 4 – 10) and time (30 – 80 min). The F-value of BBD model for RR4 removal efficiency was 185.36 (corresponding p-value < 0.0001). The results illustrated that the highest RR4 removal efficiency (70.53%) was obtained at the following conditions: adsorbent dose (1.0 g), pH 4 and time of 80 min.

**Keywords:** Chitosan; Epichlorohydrin adsorption; Reactive Red 4 dye; Box-Behnken Design

## INTRODUCTION

Environmental pollution, particularly industrial effluent, is becoming a major issue with the rapid growth of the chemical industry. Industries such as textile, paper-making and printing industries are the primary sources of contaminating the water with dyes as they used two-third of the dyes produced in the world [1]. Most of these dyes are considered to be harmful and have a complex and stable aromatic structure that makes it difficult to degrade [2]. Adsorption has been recognized to be one of the most promising and efficient techniques available for removing [3].

Chitosan (Cs) is a copolymer composed of repeated units of 2-amino-2-deoxy-D-glucopyranose units and residual 2-acetamido-2-deoxy-D-glucopyranose units [4]. Cs has a wide range of applications and uses as a biopolymer. It has been extensively studied for the removal of a range of various pollutants such as heavy metals, dyes and other industrial effluents [5]. However, its low surface area, high swelling index and solubility in various mineral acids and organic acids restricts the use of unmodified Cs as a biosorbent for removal of dyes in wastewater treatment technologies [6].

The stability of Cs in acidic environment and its mechanical properties for adsorption can be improved by crosslinking [7]. The nature of the crosslinking agent and crosslinking density play a significant role in describing the adsorption properties of chitosan-based adsorbents [5]. Various crosslinking agents such as glutaraldehyde [8], ethylene glycol diglycidyl ether [6], glyoxal [9] and epichlorohydrin [10] can be used in performing the crosslinking reaction. In this study, Epichlorohydrin (Ech) was chosen as a convenient base cross-linking agent. One of the advantages of Ech is that it does not suppress the cationic amine function of Cs, which is the main adsorption site that attracts anionic dyes during adsorption [11].

Therefore, the aim of this work is to synthesize the cross-linked chitosan-epichlorohydrin for the removal of Reactive Red 4 (RR4) from aqueous solution. Box-Behnken Design (BBD) was used to optimize the key parameters (adsorbent dose, pH and time) for the removal of Reactive Red 4 (RR4) dye by using the synthesized chitosan-epichlorohydrin (Cs-Ech). Statistical and graphical analysis of the BBD model was carried out in order to obtain the optimal conditions for effective removal of RR4 dye from aqueous solution.

## EXPERIMENTAL

### Materials

Chitosan flakes (Cs, degree of acetylation  $\geq 75$ ) was supplied by Sigma-Aldrich. Reactive Red 4 (RR4) was purchased from Aldrich Chemical (molecular weight 995.23 g mol<sup>-1</sup>; chemical formula C<sub>32</sub>H<sub>23</sub>ClN<sub>8</sub>Na<sub>4</sub>O<sub>14</sub>S<sub>4</sub>;  $\lambda_{\text{max}} = 517\text{nm}$ ). Epichlorohydrin (Ech) was purchased from Fluka. Acetic acid (CH<sub>3</sub>COOH) and sodium hydroxide (NaOH) were obtained from HmbG Chemicals. Ultra-pure water (18 M $\Omega$ /cm) was used to prepare all reagents and solutions throughout the experiment.

### Preparation of Cs-Ech

2.0 g of chitosan flakes was dissolved in 90 mL of 5% of acetic acid solution. The solution was left to stir for 24 h to allow complete dissolution of chitosan flakes. The viscous solution was beaded through a 10

mL syringe into 1000 mL of NaOH (0.5 M) under stirring. The beads were washed with distilled water several times to remove any remaining NaOH until it reaches neutral pH. The crosslinking reaction was carried out by adding 85 mL of 1% Ech solution and stirred gently for 2 h at 40°C. After that, the cross-linked Cs-Ech beads were washed again with distilled water and air dried for 24 h. The dried Cs-Ech was ground to powder form and sieved to constant particle size of  $\leq 250 \mu\text{m}$ .

### Characterization of Cs-Ech

The surface functional groups of Cs-Ech before and after adsorption of RR4 uptake have been determined by using a Fourier transform infrared (FTIR) spectrophotometer (Perkin Elmer, Spectrum RX I). The surface morphology of Cs-Ech was obtained using Hitachi TM3030Plus Scanning Electron Microscope (SEM) with an acceleration voltage of 5 kV and magnification of 5000x. The surface charge ( $\text{pH}_{\text{pzc}}$ ) was determined according to the method published by [12].

### Design of experiments

Box-Behnken Design (BBD) in Response Surface Methodology (RSM) was employed to optimize three individual variables namely adsorbent dose (A), pH (B) and time (C) for the adsorption of RR4 onto Cs-Ech. The designing and statistical analysis was performed by using Design Expert 11.0 Software (Stat-ease, Minneapolis, USA). Table 1 shows the codes and levels of the independent variables.

**Table 1:** Coded and actual variables and their levels

| Codes | Variables          | Level 1 (-1) | Level 2 (0) | Level 3 (+1) |
|-------|--------------------|--------------|-------------|--------------|
| A     | Adsorbent dose (g) | 0.5          | 1.0         | 1.5          |
| B     | pH                 | 4            | 7           | 10           |
| C     | Time               | 30           | 55          | 80           |

The experimental data were fitted to a second-order polynomial equation of quadratic order as shown in Eq. (1)

$$Y = \beta_0 + \sum \beta_i X_i + \sum \beta_{ii} X_i^2 + \sum \sum \beta_{ij} X_i X_j \quad (1)$$

where Y is the response for RR4 dye removal (%), while 0, i, ii and ij are the constant coefficient, the linear coefficient, the quadratic coefficient and the interaction coefficient, respectively.  $X_i$  and  $X_j$  are the coded values of the independent variables.

A total of 17 runs have been conducted to optimize the levels of the independent variables, namely, A: adsorbent dose (0.5 – 1.5 g), B: pH (4 – 10) and C: time (30 – 80 min). In the 250 mL of Erlenmeyer flasks containing 100 mL of RR4 dye solution, a certain amount of Cs-Ech was added. The flasks were capped and shaken continuously (100 strokes/ min) in water bath shaker (WNB7-45, Memmert,

Germany). The syringe filter (0.45 $\mu$ m) was then used to separate adsorbents from the RR4 dye solutions and the initial and final concentrations of RR4 dye were recorded using UV-Vis Spectrophotometer (HACH DR 2800) at  $\lambda_{\max}$  of 517 nm. The removal of RR4 dye (DR %) was calculated by using the following Eq. (2):

$$DR\% = \frac{(C_o - C_e)}{C_o} \times 100 \quad (2)$$

where  $C_o$  (mg/L) and  $C_e$  (mg/L) are the initial and equilibrium RR4 concentrations, respectively.

The actual BBD experimental design matrix is represented in Table 2.

**Table 2:** The 3-factors BBD matrix and experimental data for RR4 dye removal

| Run | A:Adsorbent dose (g) | B:pH | C:Time (min) | RR4 Removal (%) |
|-----|----------------------|------|--------------|-----------------|
| 1   | 0.5                  | 4    | 55           | 31.28           |
| 2   | 1.5                  | 4    | 55           | 60.19           |
| 3   | 0.5                  | 10   | 55           | 15.40           |
| 4   | 1.5                  | 10   | 55           | 23.69           |
| 5   | 0.5                  | 7    | 30           | 20.95           |
| 6   | 1.5                  | 7    | 30           | 37.00           |
| 7   | 0.5                  | 7    | 80           | 38.63           |
| 8   | 1.5                  | 7    | 80           | 66.39           |
| 9   | 1.0                  | 4    | 30           | 53.28           |
| 10  | 1.0                  | 10   | 30           | 21.92           |
| 11  | 1.0                  | 4    | 80           | 70.53           |
| 12  | 1.0                  | 10   | 80           | 43.85           |
| 13  | 1.0                  | 7    | 55           | 51.08           |
| 14  | 1.0                  | 7    | 55           | 51.99           |
| 15  | 1.0                  | 7    | 55           | 52.26           |
| 16  | 1.0                  | 7    | 55           | 51.72           |
| 17  | 1.0                  | 7    | 55           | 51.40           |

## RESULTS AND DISCUSSION

### Characterization of Cs-Ech

#### FTIR spectra

The FTIR spectra of the Cs-Ech before and after adsorption of RR4 are shown in Figure 1 (a) and (b) respectively. The spectrum of the cross-linked Cs-Ech before adsorption showed a number of absorption peaks, indicating the different types of functional groups available in them. The broad and strong peaks at  $\sim 3449\text{ cm}^{-1}$  demonstrated the presence of OH and  $\text{NH}_2$  groups,  $\sim 2300$  (stretching vibration of C-H bond) [6],  $1634\text{ cm}^{-1}$  (stretching vibration of N-H bond). The peaks at  $\sim 1386\text{ cm}^{-1}$  was associated to C-N stretching vibration and  $\sim 1112\text{ cm}^{-1}$  (C-O-C stretching of pyranose ring) [12]. After the adsorption of RR4 (Figure 1 b), the broad peak at  $\sim 3449\text{ cm}^{-1}$  shifted to  $\sim 3456\text{ cm}^{-1}$  suggesting a possible hydrogen bonding between RR4 and  $-\text{OH}$  group Cs-Ech [13]. In addition, the peak at  $\sim 2300\text{ cm}^{-1}$  corresponded to the stretching of C-H bond disappear which indicates a possible involvement of the functional group on the surface of Cs-Ech surface with RR4 molecules.

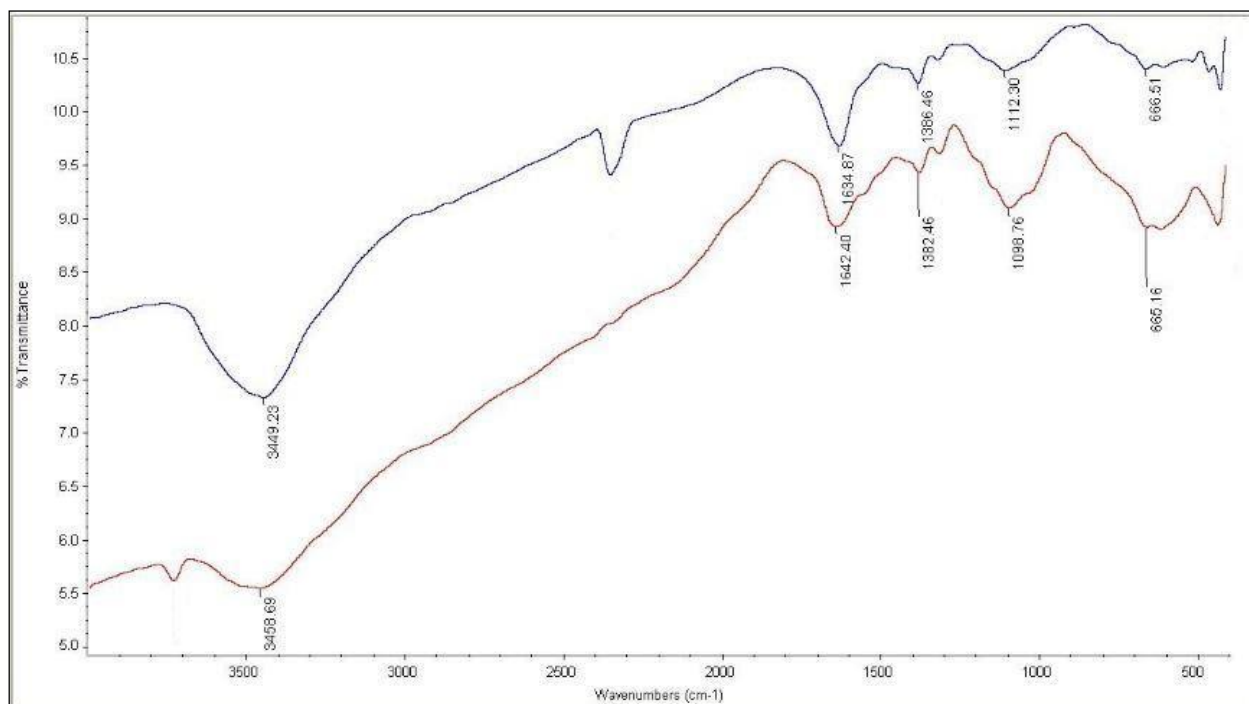


**Figure 1:** FTIR spectra of (a) Cs-Ech before adsorption, and (b) Cs-Ech after adsorption of RR4

## SEM analysis

The surface morphology of Cs-Ech was examined by Scanning Electron Microscope (SEM) and the image is shown in Figure 2. The rough and irregular surface of the Cs-Ech can be seen in the Figure 2. This rough surface shows that Cs-Ech is suitable for the adsorption of dye molecules from aqueous media [14].

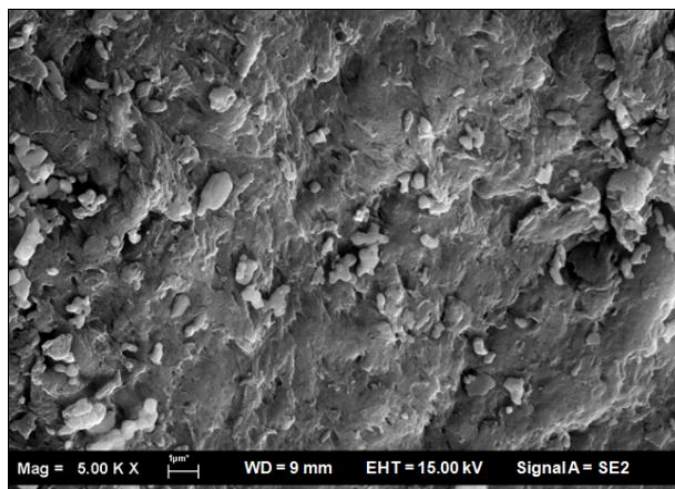


**Figure 2:** SEM image of Cs-Ech

## Response surface methodology

### Box-Behnken design

Total of 17 runs were designed by BBD (Table 2). The adsorbent dose (A), pH (B) and time (min) are the three factors that were regarded as independent process factors and the BBD approach was used to analyse the individual and interactive impact on the efficiency of the removal of RR4 as a response. The mathematical relationship between the response and the process factor was developed by using a quadratic polynomial model. The empirical relationship between the response and independent variables for Cs-Ech is expressed by Eq. (3):

$$\begin{aligned} \text{RR4 removal (\%)} = & +51.69 + 10.13A - 13.80B + 10.78C \\ & - 5.15AB + 2.93AC + 1.17BC - 12.58A^2 - 6.20B^2 + 1.90C^2 \end{aligned} \quad (3)$$

where A, B and C are the coded levels of adsorbent dose, pH and time, respectively. A positive sign signifies a synergistic impact of the factors while an antagonistic impact of the factors is shown by a negative sign [15].

Based on the coefficients of Eq (3), the parameters including adsorbent dose and time show a positive influence on the RR4 removal (%) while pH had a negative effect. It is therefore be inferred that, by increasing the adsorbent dose and time, the RR4 removal (%) increases, while the RR4 removal (%) will decrease when the pH increases [16].

### Effect of input parameters

The individual effect of the parameters studied, which includes adsorbent dose (A), pH (B) and time (C) on the removal efficiency (%) of RR4 was evaluated by perturbation plots as shown in Figure 3. The sharp curvature in curve (A) implies that RR4 removal was sensitive to this variable. The relatively sharp line of C shows the high sensitivity to change in time levels. The pH curve shows a slow curvature indicating that this factor has slight effect on the response.

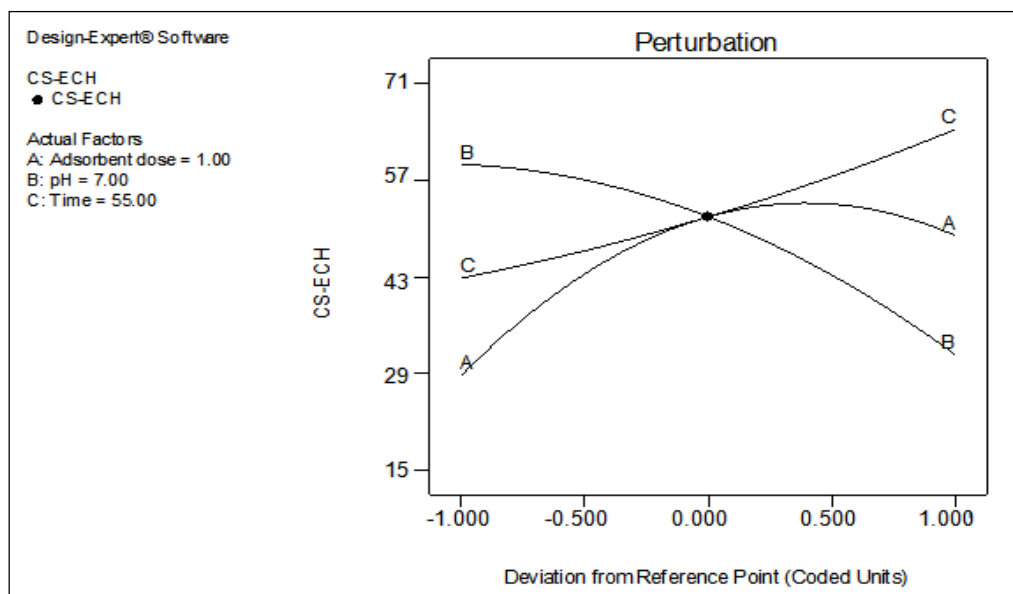


Figure 3: Perturbation plots for the RR4 removal efficiency. (A) Adsorbent dose, (B) pH and (C) time

### Analysis of variance (ANOVA)

The analysis of variance (ANOVA) verified the fitness and the significance of the model. F-values greater than five only can explain a significant response variation for various variables and combination of variable regressions [17]. The relevance of the model can be statistically valid if its p-value is less than 0.05 [18]. The F-value and p-value of the BBD model are 185.36 and  $< 0.0001$ , respectively, according to Table 3. This result shows that the model is statistically significant [19]. The chance that the F-value model large could occur due to noise is only 0.01%. Furthermore, the high correlation between the values of actual and predicted indicates that the coefficient of determination ( $R^2$ ) value (0.99) was close to one.

The terms of model with  $p\text{-value} < 0.05$  ( $\text{Prob} > F < 0.0500$ ) were significant on the RR4 removal under selected conditions.

Based on Table 3, the BBD model terms A, B, C,  $A^2$ ,  $B^2$ ,  $C^2$ , AB and AC are significant model terms. However, the model term with  $p\text{-value} > 0.05$  is insignificant and was therefore eliminated from the model in order to improve the fitting of the model.

**Table 3:** Analysis of variance (ANOVA) of the response surface quadratic model for RR4 removal efficiency

| Source            | Sum Squares | DF | Mean Square | F-value | p-value  | Remarks       |
|-------------------|-------------|----|-------------|---------|----------|---------------|
| Model             | 4318.32     | 9  | 479.81      | 185.36  | < 0.0001 | Significant   |
| A- Adsorbent dose | 820.33      | 1  | 820.33      | 316.91  | < 0.0001 | Significant   |
| B-pH              | 1524.07     | 1  | 1524.07     | 588.79  | < 0.0001 | Significant   |
| C-Time            | 929.88      | 1  | 929.88      | 359.24  | < 0.0001 | Significant   |
| $A^2$             | 695.39      | 1  | 695.39      | 268.65  | < 0.0001 | Significant   |
| $B^2$             | 161.79      | 1  | 161.79      | 62.50   | < 0.0001 | Significant   |
| $C^2$             | 15.26       | 1  | 15.26       | 5.90    | 0.0456   | Significant   |
| AB                | 106.30      | 1  | 106.30      | 41.06   | 0.0004   | Significant   |
| AC                | 34.28       | 1  | 34.28       | 13.24   | 0.0083   | Significant   |
| BC                | 5.48        | 1  | 5.48        | 2.12    | 0.1892   | Insignificant |
| Residual          | 18.12       | 7  | 2.59        |         |          |               |
| Cor Total         | 4336.44     | 16 |             | 26.37   |          |               |

Graphical methods can also be used to verify the BBD model by assessing the nature of the residuals distribution of the model and relationship between predicted and actual RR4 dye removal values. Figure 4(a) shows a normal probability plot of the residuals. The data points on this plot are reasonably close to a straight line, providing support that A, B, C,  $A^2$ ,  $B^2$ ,  $C^2$ , AB and AC are the key factors and that the basic assumptions of the analysis are satisfied [20]. The relationship between actual and predicted RR4 dye values is shown in Figure 4 (b). The model developed is adequate since the points are likely to be close to the vertical line [21].



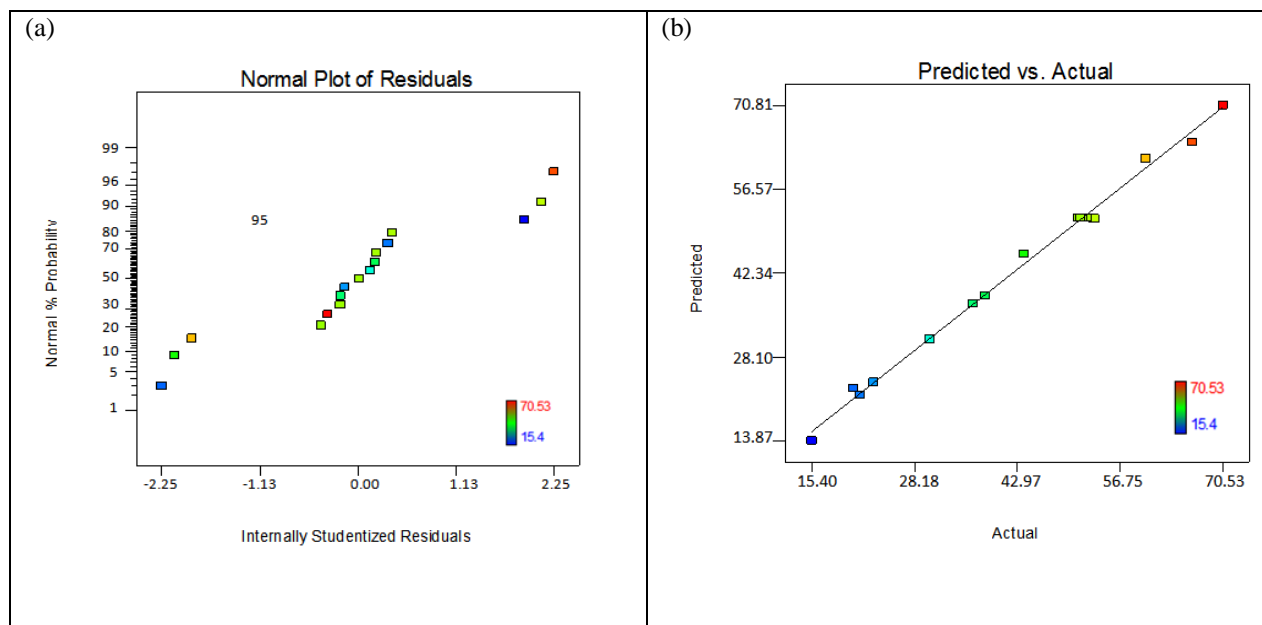


**Figure 4:** (a) Normal probability of plot of residuals for RR4 removal efficiency; (b) Plot of the relationship between the predicted and actual values of RR4 removal (%)

### Three-dimensional (3D) response surface

The interaction effect on the removal of RR4 dyes between each of two parameters was studied. The synergy between adsorbent dosage (A) and pH (B) on the removal of RR4 dye was statistically significant ( $p$ -value = 0.0004). The other input factor, time (55 min), remained constant within the experimental range. Figure 5(a) and 5(b) demonstrate the 3D surface and 2D contour of the AB interaction, respectively.

Figure 5 shows clearly that the removal of RR4 (%) increases to a certain amount with an increase of the adsorbent dosage and remained almost constant at a fixed time. Higher surface area and availability of additional adsorption site as the adsorbent dose increases can be associated with an increase of the adsorption [17]. At adsorbent dose greater than 1.25 g, the RR4 removal (%) increases slowly because the surface RR4 concentration and the solution RR4 concentration come to equilibrium with each other.

The influence of pH ranging from 4-10 on the adsorption of RR4 dyes by Cs-Ech is analysed and is shown in Figure 5. From the figure, the amount of dye adsorbed by Cs-Ech is higher at a lower pH and the efficiency of RR4 removal decrease by increasing the pH from 4-10. The  $pH_{pzc}$  of the Cs-Ech was 6.8 (Figure 6), indicating that Cs-Ech exhibit cationic characteristics. In addition, at a lower pH conditions, the amine groups of the chitosan become protonated and interact with the anionic functional groups of RR4 which then resulted to higher adsorption [22]. At pH above  $pH_{pzc}$ , the amine group of Cs began to deprotonate which led to the decreased in the positive charge density of Cs and thus reduced the

electrostatic interaction between Cs and dye molecules [13]. Therefore, the removal efficiency of RR4 dye at pH above  $pH_{pzc}$  decreases.

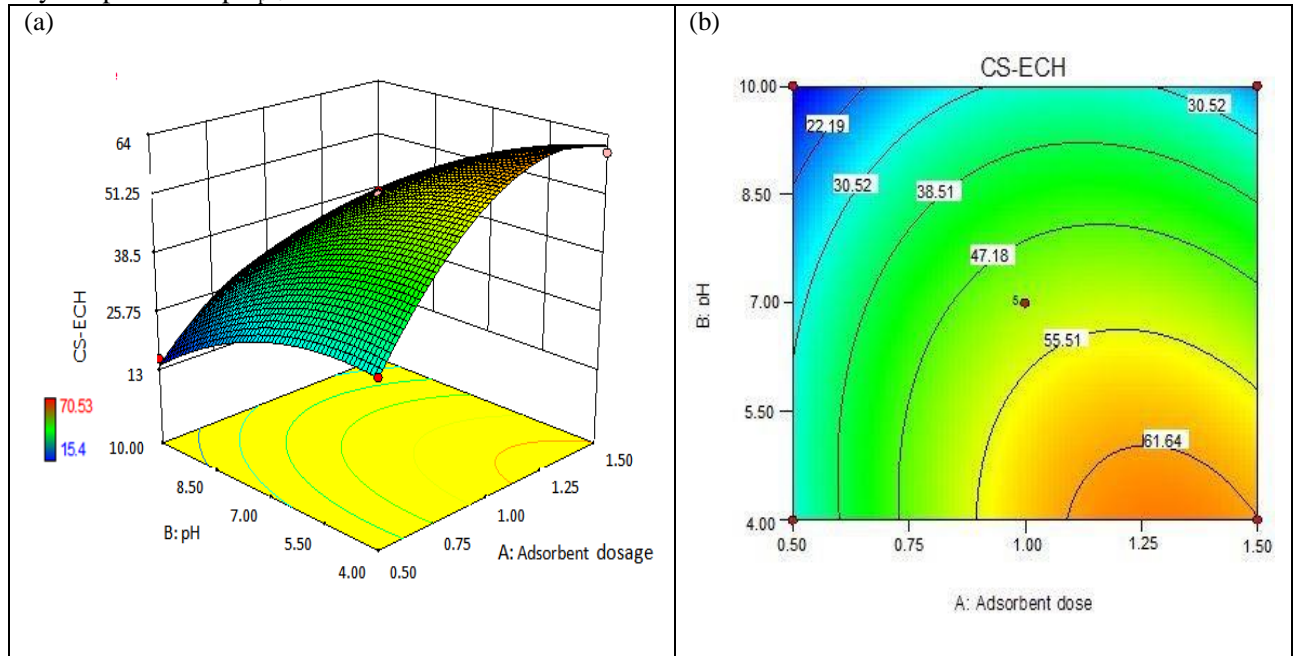


**Figure 5:** (a) 3D response surface plot; (b) contour plot for RR4 removal efficiency showing interaction between adsorbent dosage (A) and pH (B)

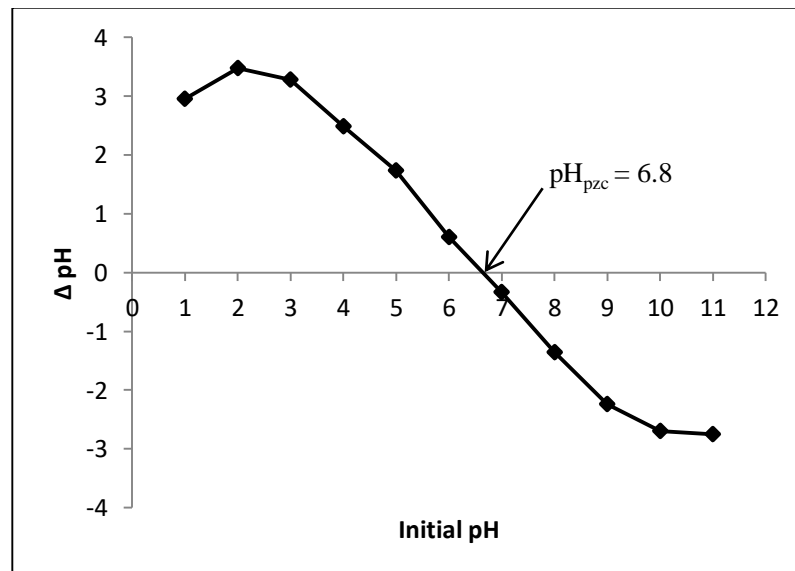


**Figure 6:**  $pH_{pzc}$  of Cs-Ech suspension

The interaction effect between adsorbent dose and time at pH = 7, on the removal of RR4 dye was statistically significant (p-value = 0.0083). Figure 7 (a) and (b) display the 3D response surface plot and 2D contour plot for the interaction of dose and time on RR4 removal (%) by Cs-Ech. It was observed from Figure 7 that by increasing the dose from 0.50 g to 1.50 g, the RR4 removal efficiency increases from 15.4% to 70.53%. This can be attributed by the availability of the exchangeable adsorption sites for the adsorption [23]. At any particular adsorbent dose, RR4 removal (%) increases with an increase in time (Figure 5). In addition, as the time increases from 30 min to 80 min, the amount of RR4 removal (%) also increases because RR4 dye molecules are able to penetrate deeper into the inner active adsorption sites of Cs-Ech when the contact time increases [24].

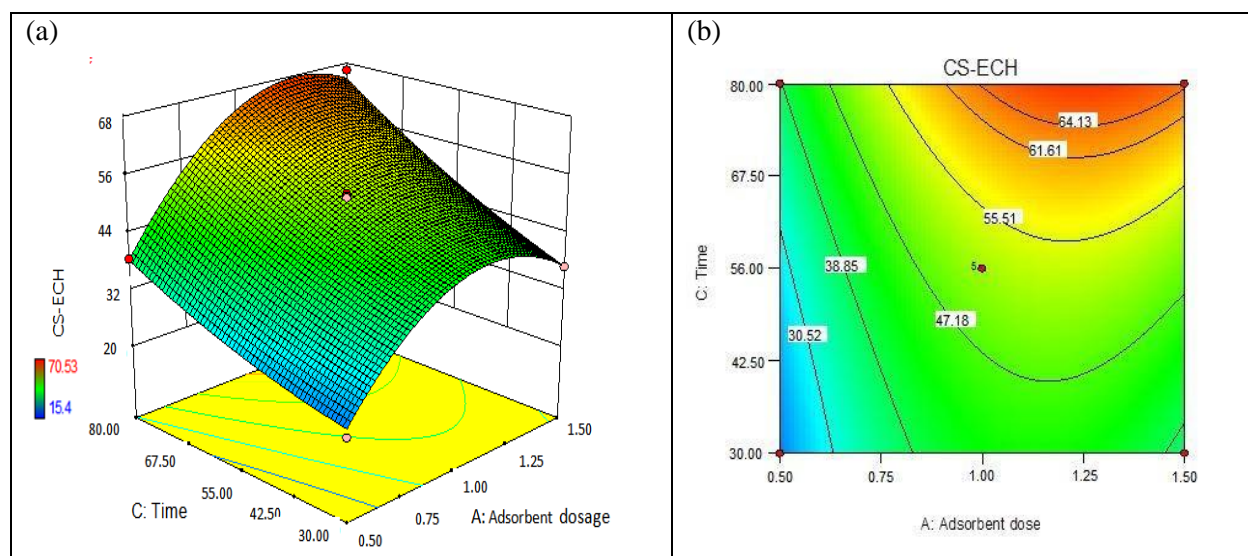


**Figure 7:** (a) 3D response surface plot; (b) contour plot for RR4 removal efficiency showing interaction between adsorbent dosage (A) and time (C)

## CONCLUSIONS

In this work, the efficiency of chitosan-epichlorohydrin (Cs-Ech) on the removal of RR4 from aqueous solution was investigated. The adsorption key parameters (adsorbent dose, pH and time) for the removal of RR4 from aqueous solution were optimized by employing Box-Behnken Design (BBD). The highest RR4 removal was obtained by simultaneous interactions between AB and AC. The best optimum conditions obtained were; adsorbent dose (1.0 g), pH ~4 and time (80 min).

## ACKNOWLEDGMENTS

The authors would like to thank Ministry of Higher Education, Malaysia for supporting this research project under fundamental research grant scheme (600-IRMI/FRGS/5/3 (340/2019); FRGS/1/2019/STG01/UiTM/02/3).

## REFERENCES

- [1]. S. Yu, J. Cui, J. Wang, C. Zhong, X. Wang, and N. Wang, "Facile fabrication of Cu (II) coordinated chitosan-based magnetic material for effective adsorption of reactive brilliant red from aqueous solution," *International Journal of Biological Macromolecules*, vol. 149, pp. 562-571, 2020.
- [2]. M. de la Luz-Asunción, E. E. Perez-Ramirez, A. L. Martinez-Hernandez, P. E. García-Casillas, J. G. Luna-Bárceñas, and C. Velasco-Santos, "Adsorption and kinetic study of Reactive Red 2 dye onto graphene oxides and graphene quantum dots," *Diamond and Related Materials*, p. 108002, 2020.
- [3]. W. Konicki, M. Aleksandrak, and E. Mijowska, "Equilibrium, kinetic and thermodynamic studies on adsorption of cationic dyes from aqueous solutions using graphene oxide," *Chemical Engineering Research and Design*, vol. 123, pp. 35-49, 2017.
- [4]. N. A. Negm, H. H. Hefni, A. A. Abd-Elaal, E. A. Badr, and M. T. Abou Kana, "Advancement on modification of chitosan biopolymer and its potential applications," *International Journal of Biological Macromolecules*, 2020.
- [5]. P. A. Nishad, A. Bhaskarapillai, and S. Velmurugan, "Enhancing the antimony sorption properties of nano titania-chitosan beads using epichlorohydrin as the crosslinker," *Journal of hazardous materials*, vol. 334, pp. 160-167, 2017.
- [6]. A. S. Abdulhameed, A. H. Jawad, and A.-T. Mohammad, "Synthesis of chitosan-ethylene glycol diglycidyl ether/TiO<sub>2</sub> nanoparticles for adsorption of reactive orange 16 dye using a response surface methodology approach," *Bioresource technology*, vol. 293, p. 122071, 2019.
- [7]. N. N. Abd Malek, A. H. Jawad, A. S. Abdulhameed, K. Ismail, and B. Hameed, "New magnetic Schiff's base-chitosan-glyoxal/fly ash/Fe<sub>3</sub>O<sub>4</sub> biocomposite for the removal of anionic azo dye: An optimized process," *International Journal of Biological Macromolecules*, vol. 146, pp. 530-539, 2020.
- [8]. E. Atangana and P. J. Oberholster, "Mathematical modeling and stimulation of thermodynamic parameters for the removal for Cr<sup>6+</sup> from wastewater using chitosan cross-linked glutaraldehyde adsorbent," *Alexandria Engineering Journal*, 2019.
- [9]. X. Li, Z. Zhang, A. Fakhri, V. K. Gupta, and S. Agarwal, "Adsorption and photocatalysis assisted optimization for drug removal by chitosan-glyoxal/Polyvinylpyrrolidone/MoS<sub>2</sub> nanocomposites," *International journal of biological macromolecules*, vol. 136, pp. 469-475, 2019.
- [10]. Y. Gutha, Y. Zhang, W. Zhang, and X. Jiao, "Magnetic-epichlorohydrin crosslinked chitosan schiff's base (m-ECCSB) as a novel adsorbent for the removal of Cu (II) ions from aqueous environment," *International journal of biological macromolecules*, vol. 97, pp. 85-98, 2017.
- [11]. T.-Y. Kim, S.-S. Park, and S.-Y. Cho, "Adsorption characteristics of Reactive Black 5 onto chitosan beads cross-linked with epichlorohydrin," *Journal of Industrial and Engineering Chemistry*, vol. 18, pp. 1458-1464, 2012.
- [12]. A. H. Jawada, N. S. A. Mubarak, and S. Sabar, "Adsorption and mechanism study for reactive red 120 dye removal by cross-linked chitosan-epichlorohydrin biobeads," *DESALINATION AND WATER TREATMENT*, vol. 164, pp. 378-387, 2019.
- [13]. M. Nawi, S. Sabar, A. Jawad, and W. W. Ngah, "Adsorption of Reactive Red 4 by immobilized chitosan on glass plates: Towards the design of immobilized TiO<sub>2</sub>-chitosan synergistic photocatalyst-adsorption bilayer system," *Biochemical Engineering Journal*, vol. 49, pp. 317-325, 2010.
- [14]. E. Binaeian, S. B. Zadvarzi, and D. Yuan, "Anionic dye uptake via composite using chitosan-polyacrylamide hydrogel as matrix containing TiO<sub>2</sub> nanoparticles; comprehensive adsorption studies," *International journal of biological macromolecules*, 2020.
- [15]. A.-T. Mohammad, A. S. Abdulhameed, and A. H. Jawad, "Box-Behnken design to optimize the synthesis of new crosslinked chitosan-glyoxal/TiO<sub>2</sub> nanocomposite: methyl orange adsorption and mechanism studies," *International journal of biological macromolecules*, vol. 129, pp. 98-109, 2019.
- [16]. A. S. Abdulhameed, A.-T. Mohammad, and A. H. Jawad, "Modeling and mechanism of reactive orange 16 dye adsorption by chitosan-glyoxal/TiO<sub>2</sub> nanocomposite: application of response surface methodology," *Desalination and Water Treatment*, vol. 164, pp. 346-360, 2019.

- [17]. M. Danish, W. A. Khanday, R. Hashim, N. S. B. Sulaiman, M. N. Akhtar, and M. Nizami, "Application of optimized large surface area date stone (*Phoenix dactylifera*) activated carbon for rhodamin B removal from aqueous solution: Box-Behnken design approach," *Ecotoxicology and environmental safety*, vol. 139, pp. 280-290, 2017.
- [18]. M. Mourabet, A. El Rhilassi, H. El Boujaady, M. Bennani-Ziatni, R. El Hamri, and A. Taitai, "Removal of fluoride from aqueous solution by adsorption on Apatitic tricalcium phosphate using Box–Behnken design and desirability function," *Applied Surface Science*, vol. 258, pp. 4402-4410, 2012.
- [19]. A. H. Jawad, A. F. Alkarkhi, and N. S. A. Mubarak, "Photocatalytic decolorization of methylene blue by an immobilized TiO<sub>2</sub> film under visible light irradiation: optimization using response surface methodology (RSM)," *Desalination and Water Treatment*, vol. 56, pp. 161-172, 2015.
- [20]. A. Jawad, "Statistical Optimization for Dye Removal from Aqueous Solution by Cross-linked Chitosan Composite," *Science Letters*, vol. 14, pp. 1-14, 2020.
- [21]. P. Tripathi, V. C. Srivastava, and A. Kumar, "Optimization of an azo dye batch adsorption parameters using Box–Behnken design," *Desalination*, vol. 249, pp. 1273-1279, 2009.
- [22]. J. Jaafari, H. Barzanouni, S. Mazloomi, N. A. Farahani, K. Sharafi, P. Soleimani, *et al.*, "Effective adsorptive removal of reactive dyes by magnetic chitosan nanoparticles: Kinetic, isothermal studies and response surface methodology," *International Journal of Biological Macromolecules*, 2020.
- [23]. J. Maity and S. K. Ray, "Chitosan based nano composite adsorbent—Synthesis, characterization and application for adsorption of binary mixtures of Pb (II) and Cd (II) from water," *Carbohydrate polymers*, vol. 182, pp. 159-171, 2018.
- [24]. I. A. Mohammed, A. H. Jawad, A. S. Abdulhameed, and M. S. Mastulia, "Physicochemical modification of chitosan with fly ash and tripolyphosphate for removal of reactive red 120 dye: Statistical optimization and mechanism study," *International Journal of Biological Macromolecules*, 2020.